Dependence of secondary-electron emission on the emergent angle of frozen-charged H^0 and H^+ projectiles penetrating a thin carbon foil

H. Ogawa,[1,*] T. Ohata,[1] K. Ishii,[1] N. Sakamoto,[1] and T. Kaneko[2]

[1]*Department of Physics, Nara Women's University, Nara 630-8506, Japan*
[2]*Department of Applied Physics, Okayama University of Science, Okayama 700-0005, Japan*

The statistical distributions of the number of secondary electrons (SEs) emitted per projectile from a thin carbon foil under irradiation with the frozen-charged H^0 and H^+ projectiles of 2.5–3.5 MeV have been measured as a function of the emergent angle of projectiles in the range from 0.0 to 2.0 mrad in every 0.5 mrad step. The measurement of SEs was carried out in the forward and the backward directions of the incident beam independently. From 0.0 mrad to ~1.0 mrad, the SE yields, that is, the mean number of emitted electrons per incident ion, increase with increasing emergent angle and tend to be saturated at larger angles. This is a common trend, regardless of incident energies and charge states of a projectile and also of emitted directions of SEs. Quantitatively, the saturated SE yields at larger angles for the H^+ penetration are about 40–50 % larger than those at 0.0 mrad. On the other hand, the corresponding relative increase for the H^0 penetration reaches as high as ~100% or more. The observed proton-hydrogen difference is well reproduced in the calculated energy losses by a Monte Carlo simulation including the impact parameter dependent stopping cross sections in a single collision of a hydrogen or a proton with a carbon atom.

PACS number(s): 79.20.Rf, 34.50.Bw, 34.50.Fa

Kinetic emission of secondary electrons (SEs) from a solid surface under fast ion bombardments has been studied intensively for a long time [1,2]. A pioneering work by Sternglass has proposed a three step model for the kinetic SE emission process. First, the creation of internal SEs via collisions of projectiles with target atoms in the solid. Second, the transport of these electrons through the bulk to the surface including higher order ionizations by those with high energies. Third, there is the transmission through the surface potential barrier [3]. Furthermore, a linear relation is proposed between the SE yields γ, i.e., the average number of the emitted electrons per projectile, and the electronic stopping power S_e of the target material [3–5]. This relation is quite understandable because the total energy per unit length deposited to the excited electrons produced in the first step should be proportional to the energy loss of the projectile. In accordance with the above prediction, approximately linear relations between γ and S_e have been observed for the proton impact on several kinds of metal over a wide energy range from a few keV to tens of MeV [2]. In this connection, the dependence of the SE emission on the projectile charge state is also an interesting subject because the energy loss of a projectile is very sensitive to its charge state. In fact, correlations between the incident charge state of projectiles and the SE yields have been reported for ions heavier than proton [6–9]. The SE yields induced by frozen charged H^0 particles have been also discussed [10].

In our previous experimental work on the emission statistics of SEs [11], the reduction factors of the forward and backward SE yields, γ_F and γ_B, induced by the frozen-charged H^0 were found to be about 0.5 and 0.35, respectively, compared with the corresponding ones induced by H^+

of the same velocity. A simple model calculation has proved that the suppression of the low-energy electron production for H^0 projectiles and the preferential forward emission of high-energy electrons make the proton-hydrogen difference in γ_B more striking. In the subsequent work [12], we have investigated the dependence of γ_F and γ_B on the emergent angle of 2.5 MeV protons transmitted through a thin carbon foil. The measured $\gamma_{F,B}$ increase with the emergent angle up to ~1 mrad and then tend to be saturated. In order to check this tendency, we carried out a Monte Carlo simulation, which took account of the impact parameter dependent energy loss in a single collision of a proton with a carbon atom [13]. Then it is confirmed that the calculated energy losses exhibit an emergent angular dependence quite similar to that of the measured SE yields.

In the present work, a similar angular dependence has been measured under the penetration of not only protons but also frozen-charged hydrogens at energies of 2.5, 3.0, and 3.5 MeV. The origin of the observed proton-hydrogen difference in the relative increases of the saturated SE yields is discussed. Furthermore, the measured SE yields are compared with energy losses calculated by a Monte Carlo simulation including the impact parameter dependent electronic stoppings of protons [13] and also of frozen-charged hydrogens.

The experiment was performed using 2.5, 3.0, and 3.5 MeV proton and hydrogen beams obtained with a 1.7 MV tandem Van de Graaff accelerator at Nara Women's University. The collimated proton or hydrogen beams were transported to a target carbon foil with the same method described in our previous papers [11,12,14]. The target foil was tilted by 45° relative to the normal angle of incidence and floated at a potential of −30 kV. A couple of grounded electrodes were placed parallel to the beam entrance (backward) and exit (forward) surfaces of the foil and 40 mm apart from the foil. The emitted electrons from the surfaces

─────────
*Corresponding author. FAX: +81-742-3380; ogawa@cc.nara-wu.ac.jp

were accelerated to the corresponding electrodes and detected each solid-state Si detector (SSD) of a 100 mm^2 sensitive area. The measurement has been carried out independently in the forward and the backward directions. By measuring the transmitted fraction of 2.5 MeV H^0, the thickness of the carbon target foil was evaluated to be 2.0±0.1 μg/cm^2 using the numerical data of the electron loss and capture cross sections involved [14]. For the proton penetration, the method of defining the emergent angle of foil-transmitted particles and of their detection were completely the same as those employed in our previous works [12,14]. We have used independently movable vertical and horizontal slits, the widths of which were about 0.3 mm. The measurement was carried out from 0.0 to 2.0 mrad at every 0.5 mrad step.

For the hydrogen measurement, however, the extremely poor counting rate at the nonzero emergent angles made this method inefficient. In order to improve the situation, we have prepared a special metal sheet, which has several almost annular-shaped apertures corresponding to each nonzero emergent angle. This slit was mounted on a movable stage placed about 1.9 m downstream of the target foil. The angular acceptance of each aperture was ±0.25 mrad. The foil-transmitted particles were magnetically analyzed and angle-resolved hydrogens were detected by a Si photodiode of 800 mm^2 sensitive area placed just behind the apertures. By employing this sheet, the measurement with the H^0 particles could be carried out up to 1.5 mrad. The fraction of projectiles, which have undergone charge exchange in the detected H^0 particles, was diminished to be less than 1%, which was evaluated from the thickness of the target foil and from the electron loss and capture cross sections involved [15]. The energy spectrum of electrons emitted per projectile was measured in coincidence with angle-resolved protons or hydrogens. The beam intensity of H$^+$ projectiles was adjusted so that the counting rate of SEs induced not by the angle-resolved protons but by the incident protons did not exceed ∼2000 cps. As for H^0 projectiles, the counting rate of projectiles was at most ∼1000 cps.

The analysis of electron energy spectra detected by the SSD was carried out in the same manner as employed in our previous works [11,12,14] on the basis of the method presented in Ref. [16]. The energy spectrum $S(E)$ can be described by the following equation:

$$S(E) = \sum_{n=1}^{n_{max}} Y_n F_n(E), \tag{1}$$

where $F_n(E)$ and Y_n denote the normalized energy distribution and the number of total events for n-electron emission per projectile, respectively. $F_n(E)$ is expressed by the superposition of $n+1$ Gaussian functions corresponding to the number of electrons backscattered through the detector surface. Several parameters, such as the electron backscattering probability at the detector surface, its K factor, the energy resolution of the SSD, and so forth included in $F_n(E)s$ were determined carefully together with each Y_n so that Eq. (1) can reproduce the observed electron energy spectrum very well. In the present analysis n_{max} the maximum number of
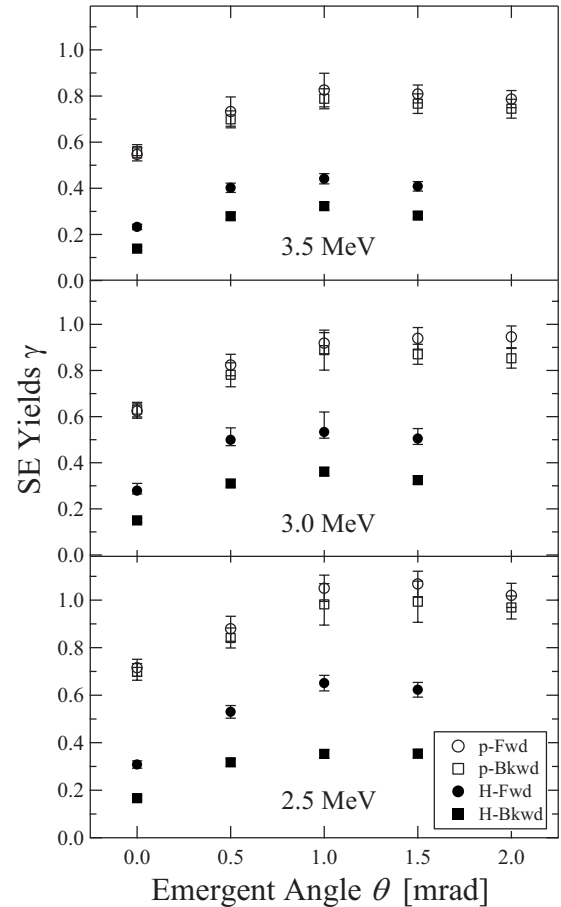

FIG. 1. The dependence of measured SE yields emitted from a carbon foil of 2.0 μg/cm^2 on the emergent angle of foil-transmitted H^0 (solid symbols) and H$^+$ (open symbols) projectiles in the frozen-charge state. Bottom, middle, and top panels are for projectiles of 2.5, 3.0, and 3.5 MeV, respectively, and circles and squares represent the results of the forward and the backward emission, respectively.

emitted SEs per projectile observed in the spectra were typically 11–13 and 13–15 for H^0 and H$^+$, respectively. Then we obtain the SE yields γ as

$$\gamma = \sum_{n=1}^{n_{max}} n W_n \quad \text{with } W_n = Y_n/N_{prj}, \tag{2}$$

where N_{prj} and W_n denote the number of detected projectiles and the probability of n-electron emission per projectile, respectively.

Figure 1 represents the observed angular dependence of the SE yields. The bottom, middle, and top panels of this figure are for projectiles of 2.5, 3.0, and 3.5 MeV, respectively. In each panel, full and open symbols refer to the H^0 and H$^+$ penetration, respectively, and circles and squares denote γ_F and γ_B, respectively. The 5% errors shown in the plots are associated with the uncertainty of the 45° tilt angle of the target. As a common behavior, irrespective of energies and charge states of a projectile, and of the emitted direction, the SE yields increase with increasing the emergent angle and tend to be saturated at angles larger than ∼1 mrad. This
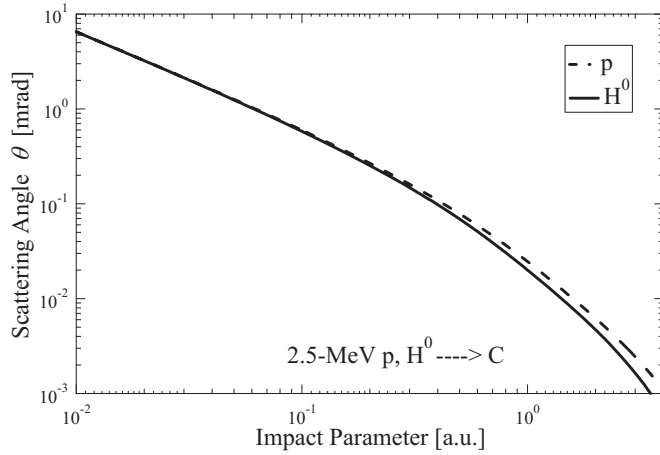
FIG. 2. The relation between the impact parameter and the scattering angle in a single collision of 2.5 MeV H^0 (solid curve) and H^+ (dashed curve) with a carbon atom through the Molière potential [17] with the Thomas-Fermi screening radius given by Eq. (3).

behavior has been already observed in our previous work under the 2.5 MeV proton incidence and a qualitative interpretation has been presented [12]. Just the same explanation can be applicable also to the observed angular dependence for the penetration of 3.0 and 3.5 MeV protons.

Curves in Fig. 2 represent the relation between the impact parameter and the scattering angle calculated in a collision of 2.5 MeV H^0 (solid curve) and H^+ (dashed curve) with a carbon atom. Here we use the Molière potential [17] with the Thomas-Fermi screening radius a_{TF} given by

$$a_{TF} = \frac{0.88534}{\{Z_T^{2/3} + (Z_p - q)^{2/3}\}^{1/2}} \quad [\text{a.u.}], \tag{3}$$

where Z_T and Z_p denote the atomic numbers of the target and the projectile, respectively, and q represents the projectile charge state. As is clear in the figure, the screening effect of its bound electron for H^0 is less effective on close collisions of $\theta \gtrsim 0.5$ mrad. Therefore, a similar angular dependence is obtained also for the H^0 penetration ($Z_p = 1$, $q = 0$). In contrast to the H^+ penetration, a prominent forward-backward difference is observed for the H^0 penetration at every angle. As is already pointed out in our previous paper [11], the suppression of the low-energy electron production for H^0 projectiles and the preferential forward emission of high-energy electrons lead to the extreme reduction of the γ_B values for H^0.

Figure 3 represents the normalized SE yields to those at 0.0 mrad. The bottom, middle, and top panels of this figure are for projectiles of 2.5, 3.0, and 3.5 MeV, respectively. Left and right parts are for the H^+ and H^0 penetration. In each panel, circles and squares represent γ_F and γ_B, respectively. Irrespective of projectile energy and emitted direction, the relative increase in the normalized SE yields for protons is saturated to 40–50 %, while for H^0 particles it amounts to as high as 100% or more. Primarily, the increase of high-energy internal SEs produced in close collisions with projectiles is considered to lead an enhancement of the SE yields at larger angles. In contrast, the production of the low-energy internal SEs, including the decay of plasmon excitations, is
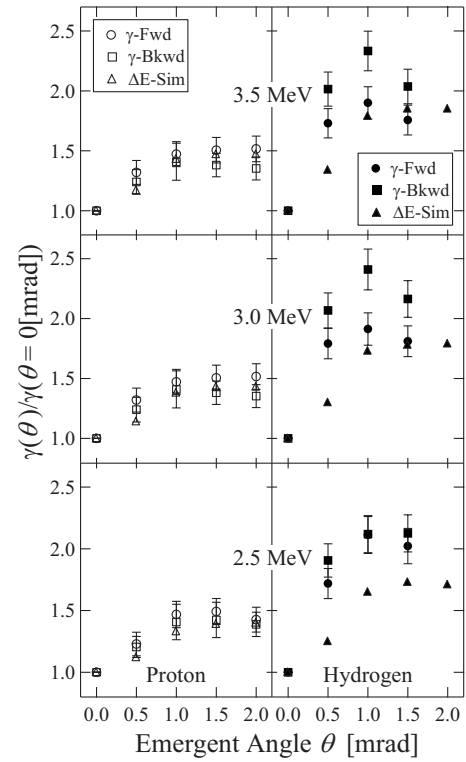

FIG. 3. The measured SE yields normalized to those at 0.0 mrad induced by frozen-charged H^0 (right part) and H^+ (left part) projectiles. Bottom, middle, and top panels are for projectiles of 2.5, 3.0, and 3.5 MeV, respectively, and circles and squares represent the results of the forward and the backward emissions, respectively. Triangles denote the corresponding energy losses calculated by a Monte Carlo simulation, which includes the impact parameter dependent energy loss in a single collision of a H^0 and a H^+ with a carbon atom [13]. Energy losses are also normalized to the SE yields at 0.0 mrad.

expected not to depend seriously on the emergent angle. Therefore, we guess that the suppression of the low-energy SE production due to the screening effect of the bound electron gives rise to an enhancement in the relative SE yields at larger emergent angles for the frozen-charged H^0 penetration.

In order to examine the validity of the above conjecture and to make a quantitative comparison with the results of the SE yields, we have carried out a Monte Carlo simulation of angular dependent energy losses under the present experimental condition. According to our previous work [12], it was found that the calculated energy losses taking account of the impact parameter dependent energy loss exhibit an angular dependence quite similar to that of the observed γ_F and γ_B. In this work, the emergent-angle dependent energy losses of frozen-charged H^0 in the target carbon foil are calculated for the first time at the incident energies of 2.5, 3.0, and 3.5 MeV in addition to those of protons. The basic data on the impact parameter dependent electronic stopping was presented by Kaneko [13]. His calculation is based on the dielectric-function method with the local-electron-density models and the electron cloud of a H^0 is described by the 1s-type wave function. It is confirmed that the stopping cross section for protons obtained by integrating over impact pa-

rameters is in good agreement with the tabulated stopping powers at this energy region [18]. The calculated stopping cross section of the graphite carbon for 10 MeV hydrogens agrees very well with the corresponding experimental result [19].

The procedures of the simulation for the proton penetration were just the same as those given in our previous papers and the details are given there [12,20]. For the H^0 incidence, the charge state of the projectile after each collision was also simulated using the impact parameter dependent charge changing probabilities calculated on the classical model by Bohr [21,22] and on the OBK theory [23] for the electron loss and capture, respectively.

Triangles in Fig. 3 represent the calculated energy losses of the frozen-charged H^+ and H^0 particles normalized to the value at 0.0 mrad. For the H^+ penetration, they agree very well with the observed angular dependence of the SE yields at each incident energy. As for the H^0 incidence, the relative increase of the simulated energy losses at larger angle is significantly larger compared with the corresponding one for the H^+ incidence. Although this behavior is compatible with the observed SE yields, the simulated energy losses slightly underestimate the relative increase of the SE yields, especially at 2.5 MeV. This simulation also shows that the charge-changed fraction in the foil-transmitted 2.5 MeV H^0 particles, which is only ~0.4% at 0 mrad, increases to ~2% at larger angles. So, the discrepancy may be partially due to the contribution from projectiles that have undergone charge exchange in the foil.

In summary, the emission statistics of the SEs from a thin carbon foil induced by frozen-charged H^0 and H^+ projectiles at the incident energy of 2.5–3.5 MeV have been measured as a function of the emergent angle of foil-transmitted particles. The obtained SE yields increase with increasing the emergent angle up to ~1 mrad, while they are saturated at larger angles. The relative increase of the SE yields at larger angles becomes more remarkable for the H^0 penetration. Monte Carlo calculations, which simulate the energy loss under the present experimental conditions, show good agreement with the measured angular dependence of the SE yields for H^+ and H^0 projectiles.

[1] J. Devooght, J. C. Dehaes, A. Dubus, M. Cailler, J. P. Ganachaud, M. Rősler, and W. Brauer, in *Particle Induced Electron Emission I*, edited by G. Höhler and E. A. Niekisch, Springer Tracts in Modern Physics Vol. 122 (Springer, Berlin, 1991).

[2] D. Hasselkamp, H. Rothard, K. O. Groeneveld, J. Kemmler, P. Varga, and H. Winter, in *Particle Induced Electron Emission II*, edited by G. Höhler and E. A. Niekisch, Springer Tracts in Modern Physics Vol. 123 (Springer, Berlin, 1991).

[3] E. J. Sternglass, Phys. Rev. **108**, 1 (1957).

[4] J. Schou, Scanning Microsc. **2**, 607 (1988).

[5] H. Rothard, C. Caraby, A. Cassimi, B. Gervais, J. P. Grandin, P. Jardin, M. Jung, A. Billebaud, M. Chevallier, K. O. Groeneveld, and R. Maier, Phys. Rev. A **51**, 3066 (1995).

[6] P. Koschar, K. Kroneberger, A. Clouvas, M. Burkhard, W. Meckbach, O. Heil, J. Kemmler, H. Rothard, K. O. Groeneveld, R. Schramm, and H.-D. Betz, Phys. Rev. A **40**, 3632 (1989).

[7] H. Rothard, K. Kroneberger, A. Clouvas, E. Veje, P. Lorenzen, N. Keller, J. Kemmler, W. Meckbach, and K. O. Groeneveld, Phys. Rev. A **41**, 2521 (1991).

[8] H. Rothard, J. Schou, and K. O. Groeneveld, Phys. Rev. A **45**, 1701 (1992).

[9] O. Benka, T. Fink, A. Schinner, and E. Steinbauer, Nucl. Instrum. Methods Phys. Res. B **125**, 41 (1997).

[10] Z. Vidović, A. Billebaud, M. Fallavier, R. Kirsch, J.-C. Poizat, and J. Remillieux, Phys. Rev. A **56**, 4807 (1997).

[11] H. Ogawa, H. Tsuchida, M. Haba, and N. Sakamoto, Phys. Rev. A **65**, 052902 (2002).

[12] H. Ogawa, H. Tsuchida, and N. Sakamoto, Phys. Rev. A **68**, 052901 (2003).

[13] T. Kaneko, Phys. Rev. A **33**, 1602 (1986).

[14] H. Ogawa, N. Fujimoto, T. Ohata, M. Nagano, K. Ishii, N. Sakamoto, and T. Kaneko, Nucl. Instrum. Methods Phys. Res. B **256**, 532 (2007).

[15] H. Ogawa, N. Sakamoto, and H. Tsuchida, Nucl. Instrum. Methods Phys. Res. B **164-165**, 279 (2000).

[16] G. Lakits, F. Aumayr, and H. Winter, Rev. Sci. Instrum. **60**, 3151 (1989).

[17] G. Molìere, Z. Naturforsch. A **3A**, 78 (1948).

[18] International Commission on Radiation Units and Measurements, ICRU Report No. 49 (International Commission on Radiation Units and Measurements, Bethesda) (unpublished).

[19] H. Ogawa, N. Sakamoto, I. Katayama, Y. Haruyama, M. Saito, K. Yoshida, M. Tosaki, Y. Susuki, and K. Kimura, Phys. Rev. A **54**, 5027 (1996).

[20] H. Ogawa, N. Sakamoto, and H. Tsuchida, Nucl. Instrum. Methods Phys. Res. B **193**, 85 (2002).

[21] N. Bohr, K. Dan. Vidensk. Selsk. Mat. Fys. Medd. **18**, 8 (1948).

[22] Y. Fujii, K. Sueoka, K. Kimura, and M. Mannami, J. Phys. Soc. Jpn. **58**, 2758 (1989).

[23] M. R. C. Mcdowell and J. P. Coleman, *Introduction to the Theory of Ion-Atom Collisions* (North-Holland, Amsterdam, 1970).